# Global Precipitation Measurement (GPM) Microwave Imager (GMI) Pre-flight Noise Diode Calibration

David Draper
Ball Aerospace & Technologies Corp
1600 Commerce St. Boulder, CO 80301; 303-939-4511
ddraper@ball.com

## ABSTRACT

The GMI employs a unique dual calibration system. Unlike other microwave imagers, the GMI noise diodes on the lower frequency channels as well as black-body hot and cold sky views providing four calibration points rather than two. The dual calibration system enables on-board trending of non-linearity, as well independent cross-checking of each calibration element for stability and anomalous behavior. One important benefit of the dual calibration system is the direct evaluation of noise diode behavior on-orbit. For systems that depend solely on noise diodes for calibration, validation of the noise diode performance has to be done vicariously, using the earth as the reference. Using GMI, noise diode performance analysis done directly using the hot load and cold sky views. This paper presents the pre-flight calibration performance of the noise diodes based on thermal vacuum measurements taken during GMI testing. We address stability of the noise diodes, and draw conclusions of on-orbit noise diode performance based on the ground measurements.

## INTRODUCTION

The Global Precipitation Measurement (GPM) Microwave Imager (GMI) program delivered the GMI Instrument to Goddard Space Flight Center early 2012. Currently, the GMI instrument is undergoing observatory-level integration and test. Goddard Space Flight Center plans to launch the GMI in 2014 aboard the GPM spacecraft with the Dual-frequency Precipitation Radar, affording better correlation of active and passive measurement techniques. The GMI will fly in a 65 degree inclination orbit and is intended to become the calibration standard for radiometer precipitation measurements[1].

The GMI is a conical scanning spaceborne radiometer. It contains thirteen channels including the frequencies 10.65 GHz, 18.7 GHz, 23.8 GHz, 36.64 GHz, 89 GHz, 166 GHz, and 183.31 GHz[2]. The calibration of the radiometer is performed via the on-orbit cold sky reflector and black-body hot load, providing two radiometric calibration points from which radiometric calibration can be performed. In addition, the lower frequency channels (10.65 GHz through 36.64 GHz) incorporate noise diodes, which allow for on-orbit determination of receiver nonlinearity and a backup calibration method[3]. The GMI instrument is shown in Figure 1.

With the dual calibration system, anomalous transient behavior in the hot load or cold sky views may be quickly identified. For instance, many previous scanning radiometers have suffered from solar intrusion into the hot load, which have caused transient calibration errors on the order of a few Kelvins at certain solar angles. With past radiometers such behavior typically takes months of data to adequately characterize, but can be immediately visible using the noise diode calibration system. This paper demonstrates using thermal vacuum calibration data how the noise diodes may be used to identify anomalous behavior of the primary calibration system. We also discuss the stability of the noise diodes throughout the GMI thermal calibration test.

**Figure 1: GMI Instrument**

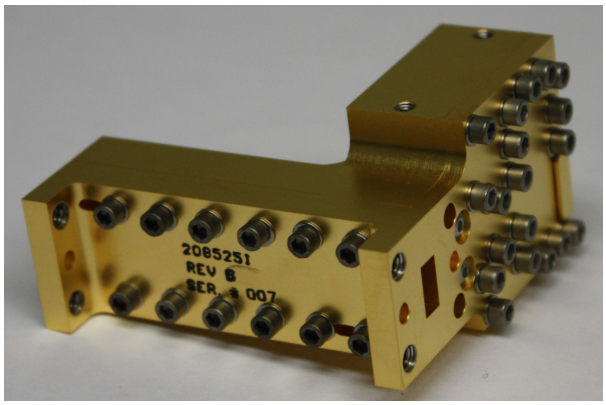


**Figure 2: GMI 36 GHz Noise Source**

## NOISE DIODES AS A BACKUP CALIBRATION SYSTEM

One of the 36 GHz noise source assemblies including the noise diode and waveguide coupler is shown in Figure 2. The noise diodes operate during the calibration view every other scan providing four calibration points: 1) cold, 2) cold + noise, 3) hot, 4) hot + noise. The baseline GMI calibration scheme uses the hot load and cold sky view along with the ground-determined non-linearity to relate observed counts to antenna brightness temperature. Calibration is performed using the radiometric transfer function (RTF),

$$T_a = T_c + \frac{C_s - C_c}{g} + u\frac{(C_s - C_c)(C_s - C_h)}{g^2} \qquad (1)$$

where

- $T_c$ and $T_h$ is the cold and hot view brightness temperatures
- $C_s$, $C_c$ and $C_h$ are the scene counts, hot counts, and cold counts respectively.
- $g = (C_h - C_c)/(T_h - T_c)$ is the gain calculated between the two calibration views
- $u = 4T_{nl}/(T_h - T_c)^2$ is the normalized non-linearity that has been characterized beforehand.
- $T_{nl}$ is the maximum non-linearity in Kelvin between the hot and cold calibration views.

In nominal conditions, the four calibration points allow determination of two other parameters: the excess temperature of the noise diodes and the non-linearity. Solving the RTF for the two noise diode views, the noise diode excess temperature can be monitored using the following equation,

$$T_{nd} = [T_h - T_c]\frac{x_{cn}(x_{hn} - x_{hn}^2) - (x_{hn} - 1)(x_{cn} - x_{cn}^2)}{x_{hn} - x_{cn} + x_{cn}^2 - x_{hn}^2} \qquad (2)$$

where

- $x_{cn} = (C_{cn} - C_c)/(C_h - C_c)$
- $x_{hn} = (C_{hn} - C_c)/(C_h - C_c)$
- $C_{cn}$ and $C_{hn}$ are the cold + noise and hot + noise counts.

Likewise, the non-linearity can be monitored using the following equation,

$$T_{nl} = [T_h - T_c]\frac{x_{hn} - x_{cn} - 1}{4(x_{hn} - x_{cn} + x_{cn}^2 - x_{hn}^2)}. \qquad (3)$$

On orbit, the noise diode excess temperature and non-linearity will be trended as a function of temperature.

Once the noise diodes have been trended on-orbit as a function of the noise diode physical temperature, the cold and cold + noise views can be used as a backup method to calibrate the instrument,

$$T_{a1} = T_c + \frac{C_s - C_c}{g_1} + u\frac{(C_s - C_c)(C_s - C_{cn})}{g_1^2} \qquad (4)$$

where $g_1 = (C_{cn} - C_c)/T_{nd-trended}$. Likewise, the hot and hot + noise views can be used to calibrate the instrument,

$$T_{a2} = T_h + \frac{C_s - C_h}{g_2} + u\frac{(C_s - C_h)(C_s - C_{hn})}{g_2^2} \qquad (5)$$

where $g_2 = (C_{hn} - C_h)/T_{nd-trended}$.

The hot and cold-view brightness temperatures can be calculated indirectly by using Equations (4) and (5) over the calibration fields of view. If the predicted hot load or cold sky temperatures from Equations (4) and (5) are in error from those used in the RTF, a transient event may have occurred. In this case, the result of Equations (4) or (5) can be used as backup calibration over the earth view[4].

## GMI CALIBRATION TEST RESULTS

The GMI ground calibration test was performed as part of the GMI thermal vacuum test program. During the calibration test, the GMI instrument viewed two external blackbody targets: a cold target cooled near liquid nitrogen temperature, and a variable target that

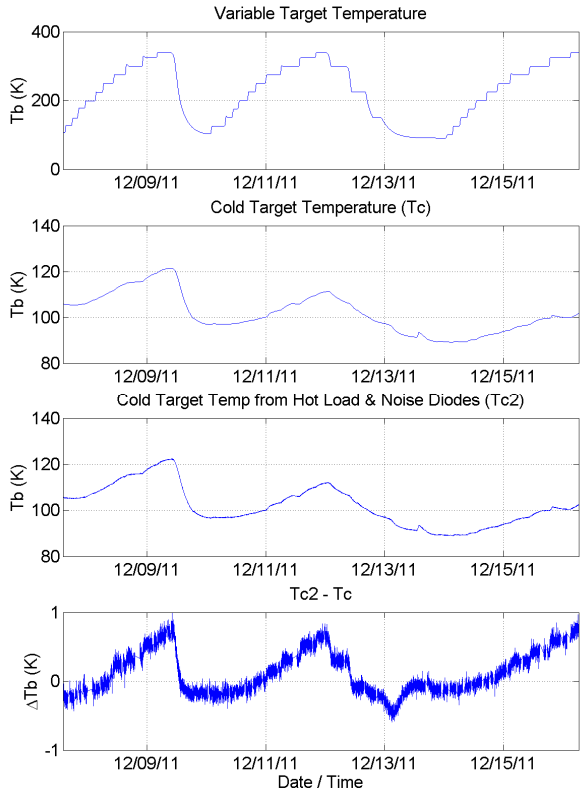


**Figure 3: Top: Variable target temperature over the duration of the GMI calibration test. 2nd from Top: Cold target-measured brightness temperature using PRTs in the target. 3rd from Top: GMI-measured cold target brightness temperature (36 GHz) using the hot load and noise diodes as calibration references Bottom: Difference between cold target temperature and the GMI-measured cold target brightness temperature**

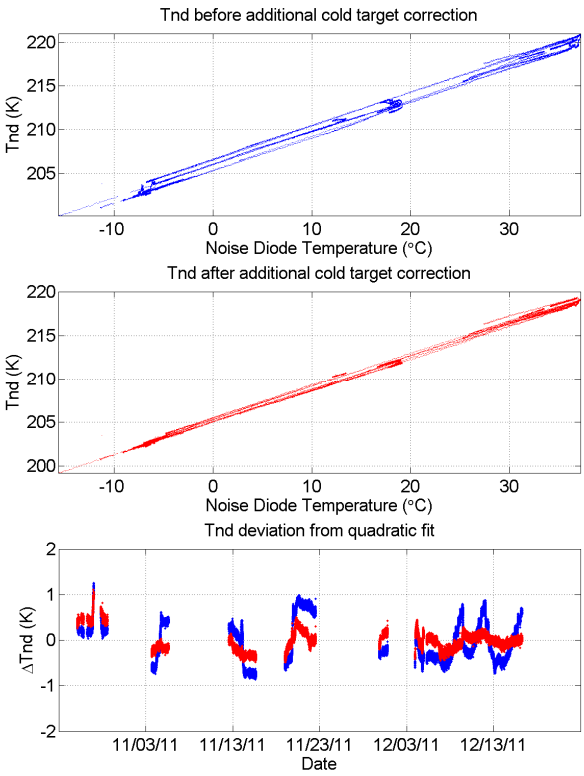


**Figure 4: Top: Noise Diode Excess Temperature as a function of Noise Diode Temperature. Middle: Noise diode excess temperature after the additional cold target correction. Bottom: Noise diode excess temperature deviation from quadratic fit**

transitioned in temperature between about 100K and 340K. The cold target replaced the cold sky view and the variable target was used to simulate the earth-scene view. The two targets were positioned in direct line-of-sight of the feedhorns and provided a method of comparing instrument performance to an external calibration system.

The GMI thermal calibration test afforded trending of the noise diode excess temperature over the physical temperature of the noise diodes using equation (2). The noise diodes excess temperature is fit with a second-order polynomial to allow determination of the noise diode excess temperature at an arbitrary noise diode physical temperature.

The thermal vacuum test provides an excellent way to demonstrate the GMI dual calibration system. A difficulty with the calibration test was that the external cold calibration target exhibited thermal gradients due to conduction issues between the target and its thermal control system. The cause of the issue is well understood and will be fixed for future instruments. The residual error associated with the cold target can be identified using the hot and hot + noise measurements.

Figure 3 shows the variable target temperature, the cold target temperature $T_c$, and the cold target temperature measured by the GMI using the hot and hot + noise views to perform calibration $T_{c2}$. The difference between the $T_c$ and $T_{c2}$ is shown in the bottom plot of Figure 2. In this case, the cold target exhibits larger-than-expected gradients induced by coupling with the variable target through the instrument top deck. As the variable target increases in temperature, the cold target also increases in temperature with corresponding greater error due to gradients induced into the cold target. This effect is removed by appropriately scaling the thermal gradient correction used to determine $T_c$[5]

**Table 1: Estimated stability of the GMI noise diodes. All numbers are 3-sigma**

| Channel | Tnd Stability (Estimated w/o Cold Correction) | Tnd Stability (Estimated w/ Cold Correction) |
|---|---|---|
| 10.65 GHz V | 2. 6 K | 2.6 K |
| 10.65 GHz H | 1.2 K | 1.0 K |
| 18.7 GHz V | 1.7 K | 0.4 K |
| 18.7 GHz H | 1.7 K | 0.4 K |
| 23.8 GHz V | 1.4 K | 0.4 K |
| 36.64 GHz V | 1.6 K | 0.8 K |
| 36.64 GHz H | 1.4 K | 0.7 K |

## GMI NOISE DIODE STABILITY

In order to use the noise diodes as a backup calibration source on-orbit, it is required that the noise diode excess temperature be sufficiently stable as to adequately predict the noise diode excess temperature when the hot or cold target cannot be used for direct calibration. The ground calibration can be used to assess the stability of the noise diodes by demonstrating how well a 2$^{nd}$-order polynomial may be used to predict the noise diode excess temperature over the duration of the thermal vacuum test.

Figure 4 shows the 36 GHz V-pol noise diode excess temperature as a function of noise diode physical temperature prior to and after correcting for the cold target gradients identified in the previous section. For this particular noise diode, The quadratic fit can adequately represent the noise diode temperature to within about 0.7K over the duration of the GMI thermal vacuum testing. The 3-sigma RMS error of all noise diode excess temperatures from the quadratic fits are given in Table 1. In general, the physical temperature of the noise diodes can be used to predict the excess temperature towithin 1K for all noise diodes except 10.65 GHz V-pol, which exhibited some noise diode drift over the duration of the test. For this channel, there may be some initial drift on orbit that will occur. We expect that the error due to the 10.65 GHz V-pol noise diode will stabilize after launch, and will be trended to within the same stability as the H-pol noise diode.

## CONCLUSION

The noise diodes on GMI will serve as a diagnostic tool to identify transient anomalous behavior of the GMI primary calibration system. It will also be used to trend non-linearity on the low frequency channels over the life of the instrument. The thermal vacuum test results show that the excess temperature of the noise diodes should be predictable to within about 1K, with 0.4K performance for the 18 and 23 GHz channels. Only the 10 GHz V-pol noise diode exhibited noticeable drift during the GMI thermal vacuum test. Based on other instruments with noise diodes, we expect this drift to settle out on orbit.


1. "Global Precipitation Measurement," [Online]. Available: http://pmm.nasa.gov/GPM. [Accessed: Feb 08, 2012].
2. D. A. Newell e*t al.*, "GPM microwave imager instrument design and predicted performance," in Proc. IGARSS, 2007, pp. 4426–4428.
3. J. B. Sechler, "GPM microwave imager selected calibration features and predicted performance," in Proc. IGARSS, 2007, pp. 5237–5239.
4. T. Meissner, and F.J. Wentz, "GMI Calibration Algorithm and Analysis Theoretical Basis Document", Remote Sensing Systems, Santa Rosa, CA, Rep. 051707, 2012.
5. D. W Draper, D. A. Newll, D.A. Teusch and P.K. Yoho, "Global Precipitation Measurement Microwave Imager Prelaunch Hot Load Calibration," *Trans. Geosci. Remote Sens.,*vol. PP, No. 99, pp. 1-12, 2013.